

Communication

# Highly Efficient Synthesis of Cinnamamides from Methyl Cinnamates and Phenylethylamines Catalyzed by Lipozyme<sup>®</sup> TL IM under Continuous-Flow Microreactors

Lihua Du <sup>1,\*</sup>, Lingyan Zheng <sup>1</sup>, Yue Pan <sup>1</sup>, Zhikai Sheng <sup>1</sup>, Shiyi Zhang <sup>1</sup>, Hang Lin <sup>1</sup>, Aoying Zhang <sup>1</sup>, Hanjia Xie <sup>1</sup> and Xiping Luo <sup>2,\*</sup><sup>1</sup> College of Pharmaceutical Science, Zhejiang University of Technology, Hangzhou 310014, China<sup>2</sup> Zhejiang Provincial Key Laboratory of Chemical Utilization of Forestry Biomass, Zhejiang A&F University, Hangzhou 311300, China

\* Correspondence: orgdlh@zjut.edu.cn (L.D.); luoxiping@zafu.edu.cn (X.L.); Tel.: +86-189-690-693-99 (L.D.)

**Abstract:** While a few derivatives of cinnamamides exhibited anti-inflammatory and/or analgesic activity, in this study, we developed a highly efficient method for the synthesis of cinnamamides from methyl cinnamates and phenylethylamines catalyzed by Lipozyme<sup>®</sup> TL IM in continuous-flow microreactors. The reaction parameters and broad substrate range of the new method was studied. Maximum conversion (91.3%) was obtained under the optimal condition of substrate molar ratio of 1:2 (methyl 4-chlorocinnamate: phenylethylamine) at 45 °C for about 40 min. The remarkable features of this work include short residence time, mild reaction conditions, easy control of the reaction process, and that the catalyst can be recycled or reused, which provide a rapid and economical strategy for the synthesis and design of cinnamide derivatives for further research on drug activity.

**Keywords:** enzymatic synthesis; cinnamamides; continuous-flow reaction technology; continuous-flow microreactor; ammonolysis reaction



**Citation:** Du, L.; Zheng, L.; Pan, Y.; Sheng, Z.; Zhang, S.; Lin, H.; Zhang, A.; Xie, H.; Luo, X. Highly Efficient Synthesis of Cinnamamides from Methyl Cinnamates and Phenylethylamines Catalyzed by Lipozyme<sup>®</sup> TL IM under Continuous-Flow Microreactors. *Catalysts* **2022**, *12*, 1265. <https://doi.org/10.3390/catal12101265>

Academic Editors: Francesca Raganati and Alessandra Procentese

Received: 16 September 2022

Accepted: 11 October 2022

Published: 18 October 2022

**Publisher's Note:** MDPI stays neutral with regard to jurisdictional claims in published maps and institutional affiliations.



**Copyright:** © 2022 by the authors. Licensee MDPI, Basel, Switzerland. This article is an open access article distributed under the terms and conditions of the Creative Commons Attribution (CC BY) license (<https://creativecommons.org/licenses/by/4.0/>).

## 1. Introduction

The discovery of novel anti-inflammatory agents derived from natural active products has attracted a lot of attention from medicinal chemists. Cinnamic acid is a natural organic acid in plants with high safety and a variety of pharmacological activities, such as antioxidant, antimicrobial, anticancer, and anti-inflammatory activities [1–5]. Due to their common occurrence in plants and their low toxicity, cinnamic acid derivatives have been evaluated as pharmacologically active compounds [6]. Among the derivatives, cinnamamides constitute an interesting scaffold within medicinal chemistry; thus, they have been incorporated in several synthetic compounds with therapeutic potentials including neuroprotective, anti-microbial, anti-tyrosinase, and anti-inflammatory properties (Figure 1) [7–11]. Cinnamoyl phenylethylamine derivative is a class of compounds with important biological activity in cinnamide compounds. Additionally, the phenolic hydroxyl group on the benzene ring enhances the effect of inhibiting the expression of P-selectin, tyrosinase, and cyclooxygenase [11,12]. Cinnamoyl tyramine inhibits the expression of cyclooxygenase II [13] and p-coumarinyl tyramine inhibits yeast  $\alpha$ -glucosidase [14] (Figure 1).

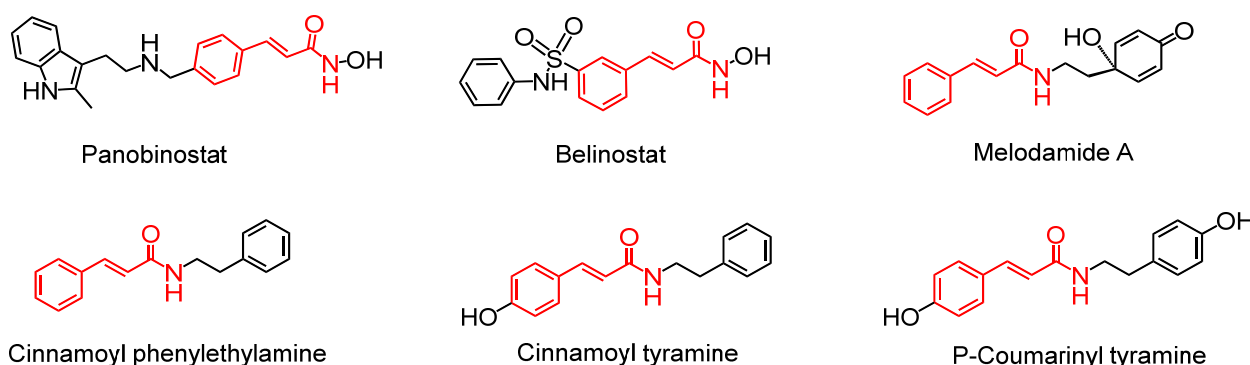


**Figure 1.** Structures of cinnamamide compounds with potential drug activities.

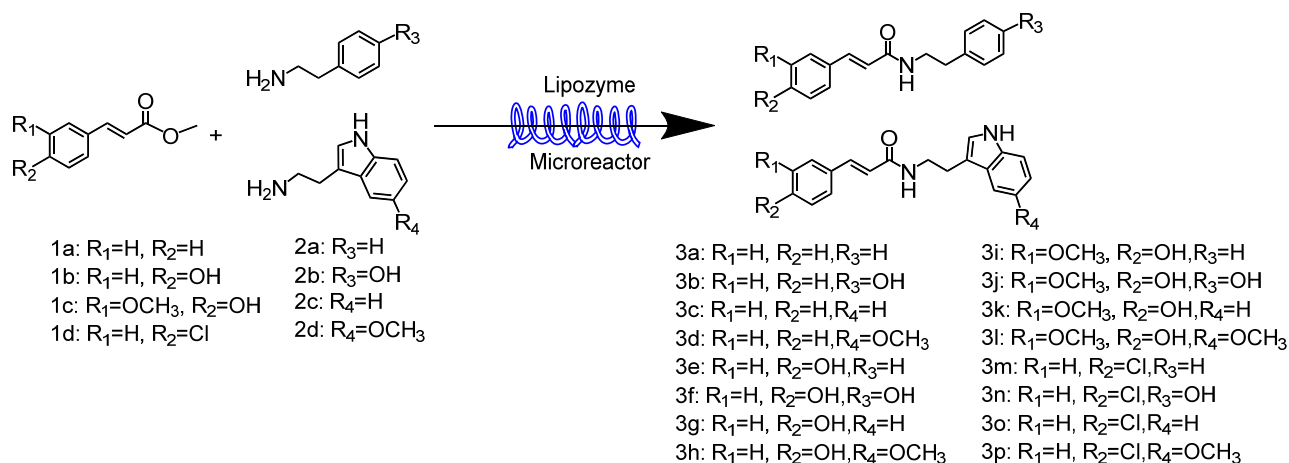
Construction of amide bonds is the key to the synthesis of cinnamamide derivatives. Traditional chemical synthesis always used condensation reagents such as 2-ethoxy-1-ethoxycarbonyl-1, 2-dihydroquinoline (EEDQ), dicyclohexylcarbodiimide (DCC) or triazine reagents to synthesize cinnamamide derivatives in *N,N*-dimethylformamide (DMF), tetrahydrofuran (THF) or pyridine [12,15–19]. However, these methods have problems such as environmental pollution, waste of energy, complexity of recycling and disposal, and may even cause allergic reactions [20–24]. In recent years, a number of new chemical catalysts for amide bond synthesis have been reported, such as iron catalysts, boron catalysts, aluminum catalysts, diacetoxyiodobenzene, and 5-nitro-4,6-dithiocyanatopyrimidine (NDTP), but they also suffered from high temperatures, complicated post-treatment, long reaction times or complicated and toxic catalyst preparation [25–29]. So, it is urgent to develop a highly efficient green technology for the synthesis of cinnamamide derivatives.

Biocatalysis, using enzymes for organic synthesis, has emerged as a powerful tool for the synthesis of active pharmaceutical ingredients [30,31]. Enzymes are employed to enable shorter, more efficient, and more sustainable alternative routes toward small-molecule active pharmaceutical ingredients and are additionally used to perform standard reactions in active pharmaceutical ingredients synthesis more efficiently [32–34]. For example, recently, an evolved *E. coli* cytidine deaminase was used for a simple enzyme-mediated transformation, paving the way for a total greener synthesis of the COVID-19 antiviral Molnupiravir [35]. Lipozyme<sup>®</sup> TL IM is a commercial heterogeneous biocatalyst supplied by Novozymes prepared via physical adsorption of the lipase from *Thermomyces lagunosus* on silica gel particles with a catalyst reactivity of 250 IUN·g<sup>-1</sup> [36]. The development and attributes of Lipozyme<sup>®</sup> TL IM established the industrial applications for immobilized enzymes, including interesterification of food fats and oils [37,38] and development of biodiesel [39] and lipophilic antioxidants [40,41].

Compared with the traditional chemical synthesis of cinnamamides, there are relatively few studies on enzyme-catalyzed synthesis of cinnamamide derivatives. Novozym<sup>®</sup> 435 was used to catalyze the synthesis of coumaroyltyramine derivatives from hydroxycinnamate and phenylethylamines in methyl *tert*-butyl ether (MTBE) for about 24 h, and 65–93% yields of coumaroyltyramine derivatives were obtained [42]. However, enzymatic chemical reaction also has some shortcomings, such as requiring a long reaction time to obtain the desired yield. In addition, the enzymes that can be used for the synthesis of cinnamamide derivatives need to be further developed.

How to explore enzyme-catalyzed cinnamamide derivatives' synthesis reactions while improving the efficiency of traditional enzyme catalytic reactions? We think of continuous-flow biocatalysis technology as a solution. In a continuous reactor, the substrates are pumped through the reactor, and the product is collected continuously. This set up improves mass transfer, shortens reaction time, and inhibits the occurrence of side reactions effectively [43–47]. The use of Lipozyme<sup>®</sup> TL IM has received significant attention due to its easy recovery from the reaction mixture and recycling, relative inexpensiveness, and the fact that it is suitable for developing continuous-flow processes [48,49]. So, in this

work, we developed a highly efficient method for the synthesis and design of cinnamide derivatives catalyzed by Lipozyme<sup>®</sup> TL IM in continuous-flow microreactors (Scheme 1). To the best of our knowledge, this is the first description of the highly efficient synthesis of cinnamides from methyl cinnamates and phenylethylamines catalyzed by Lipozyme<sup>®</sup> TL IM under continuous-flow microreactors. The reaction parameters and broad substrate range of the new method was studied. The reaction conditions were optimized with the choice of mild temperatures and environmentally friendly solvents. At the same time, the reaction time and economic cost were saved. It is hoped to provide a rapid strategy for the synthesis and design of cinnamide derivatives for further research on drug activity.

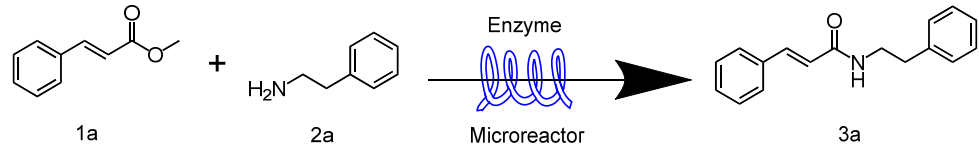


**Scheme 1.** Synthesis and design of cinnamide derivatives catalyzed by Lipozyme<sup>®</sup> TL IM in continuous-flow microreactors.

## 2. Results

### 2.1. Effect of Reaction Media and Catalyst

Reaction media and catalyst are important factors in enzymatic reactions. During our research on cinnamide derivatives' synthesis reaction from methyl cinnamate and phenylethylamines catalyzed by enzyme in continuous-flow microreactors, methyl cinnamate (1a) and phenylethylamine (2a) were selected as the model reaction. First, we performed a blank control experiment without the enzyme and found that reactions did not occur. Then, we screened the enzyme and solvent species, chose Lipozyme<sup>®</sup> TL IM from *Thermomyces lanuginosus* and Subtilisin<sup>®</sup> from *Bacillus licheniformis* as a comparison, and *tert*-amyl alcohol, acetonitrile, DMSO, DMF, *tert*-butanol, and *n*-hexane as another control group. Different enzymes have various resistance levels in different reaction systems [50]. The results are shown in Table 1; Lipozyme<sup>®</sup> TL IM and *tert*-amyl alcohol can catalyze the reaction with a higher yield (Table 1, entry 1). For the synthesis of *N*-phenethylcinnamide catalyzed by Lipozyme<sup>®</sup> TL IM, a moderate log P solvent will better promote the reaction. Neither too high nor too low reactions can be carried out. Therefore, Lipozyme<sup>®</sup> TL IM and *tert*-amyl alcohol were selected to synthesize cinnamide derivatives from methyl cinnamates and phenylethylamines under continuous-flow microreactors.

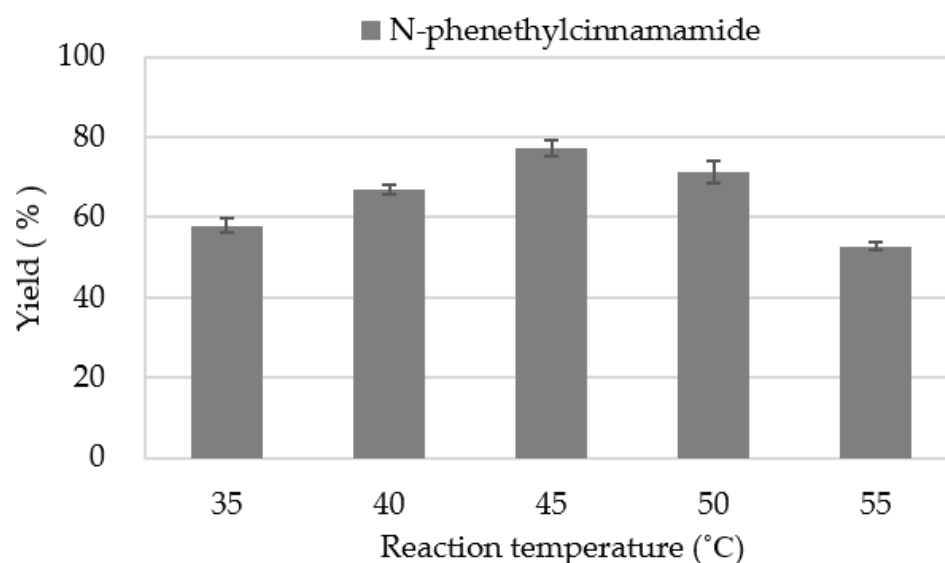
**Table 1.** The effect of reaction media and catalyst on the enzymatic synthesis of N-phenethylcinnamamide in continuous-flow microreactors <sup>a</sup>.


Entry	Solvent	Catalysts	Log P	Yield <sup>b</sup> (%)
1	<i>tert</i> -amyl alcohol	Lipozyme <sup>®</sup> TL IM	1.04	71.2 ± 1.5
2	<i>tert</i> -butanol	Lipozyme <sup>®</sup> TL IM	0.51	36.2 ± 0.8
3	acetonitrile	Lipozyme <sup>®</sup> TL IM	−0.33	33.5 ± 1.1
4	<i>n</i> -hexane	Lipozyme <sup>®</sup> TL IM	3.9	n.d.
5	DMF	Lipozyme <sup>®</sup> TL IM	−1.0	n.d.
6	DMSO	Lipozyme <sup>®</sup> TL IM	−1.3	n.d.
7	<i>tert</i> -amyl alcohol	Subtilisin <sup>®</sup>	1.04	n.d.
8	<i>tert</i> -amyl alcohol	None	1.04	n.d.

<sup>a</sup> Reaction conditions: feed 1, 5.0 mmol methyl cinnamate (1a) dissolved in 10 mL *tert*-amyl alcohol, feed 2, 10.0 mmol phenylethylamine (2a) dissolved in 10 mL *tert*-amyl alcohol, Lipozyme<sup>®</sup> TL IM (catalyst reactivity: 250IU·g<sup>−1</sup>) 0.87 g, flow rate 20.8 μL min<sup>−1</sup>, 30 min residence time at 50 °C. <sup>b</sup> Isolated yield. Yield: 100 × (actual received quantity/ideal calculated quantity). The data are presented as average ± SD of triplicate experiments.

## 2.2. Effect of Reaction Temperature

In biocatalysis reactions, reaction temperature affects the catalytic activity of enzymes and the thermodynamic equilibrium of the reaction. Using Lipozyme<sup>®</sup> TL IM as catalyst, flow reaction was carried out in *tert*-amyl alcohol at reaction temperatures of 30 °C to 55 °C for 30 min. With the rise in temperature, there was an increased rate of diffusion since the viscosity of the system was lowered so that mass transfer between the enzyme and the substrate may occur more easily. Moreover, the increase in temperature increased the kinetic energy of the molecules that led to faster and efficient collisions [51,52]. As shown in the Figure 2, when the reaction temperature was 45 °C, the best yield was obtained. However, it is best to avoid temperatures above 45 °C because an excessive increases in temperature can cause irreversible denaturation of the enzyme and a sharp decrease in enzyme activity [53].

**Figure 2.** The effect of reaction temperature on the synthesis of N-phenethylcinnamamide catalyzed by Lipozyme<sup>®</sup> TL IM in continuous-flow microreactors.

### 2.3. Effect of Substrate Ratio

Methyl cinnamate contains C=C double bonds, which can generate the formation of a side-product resulting from an aza-Michael addition [26,54]. So, a lower concentration of methyl cinnamate inhibited the by-reaction effectively. At the same time, the amidation reaction was a reversible reaction. With the increase in the substrate concentration of the amine, the thermodynamic equilibrium shifted in a direction favorable to the formation of N-phenethylcinnamamide. As seen in Figure 3, a maximum yield of 77.2% was obtained when the molar ratio (methyl cinnamate: phenylethylamine) was 1:2. However, when the molar ratio was increased further, there was a negative impact on the conversion rate. Excessive concentration of the substrate increased the viscosity of the solvent, interfered with mass transfer, changed the polarity of the solvent, and affected the activity of the enzyme, while reducing the economic efficiency [41].

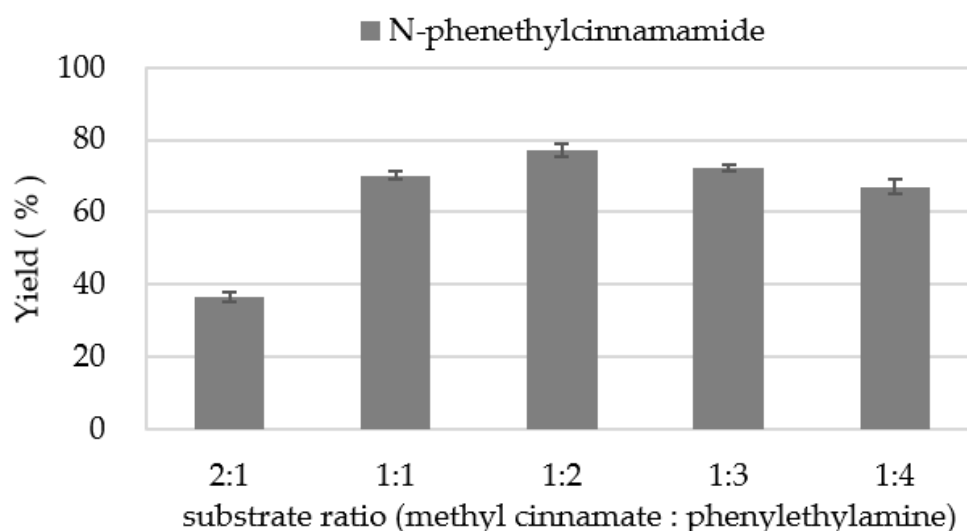


**Figure 3.** The effect of substrate ratio (methyl cinnamate: phenylethylamine) on the synthesis of N-phenethylcinnamamide catalyzed by Lipozyme<sup>®</sup> TL IM in continuous-flow microreactors.

### 2.4. Effect of Residence Time

Residence time is an important parameter affecting the conversion of reaction. We designed reactions from 20 to 50 min to investigate the effect of residence time on the reaction. As we can see from Figure 4, the optimum yield was reached within 40 min at a flow rate of 15.6  $\mu\text{L}/\text{min}^{-1}$ . Therefore, we chose 40 min as the optimal residence time for further research on the synthesis of cinnamamide derivatives under continuous-flow microreactors.

### 2.5. The Effect of Enzyme Reusability

The reusability of Lipozyme<sup>®</sup> TL IM was investigated under optimal conditions. The catalytic activity of the biocatalyst remained practically unaltered in the first two cycles, and after that, a slight decrease in activity could be detected. Additionally, after 8 catalytic cycles of the same enzyme sample, it was found that the catalytic yield of the last catalysis could still reach 46.7% (Figure 5). Such decreased activity after successive reaction cycles could be due to the desorption of immobilized lipase during the continuous flow. In addition, the accumulation of residual starting material and/or products remaining in the biocatalyst microenvironment might also lead to enzyme inactivation [49,53,55].

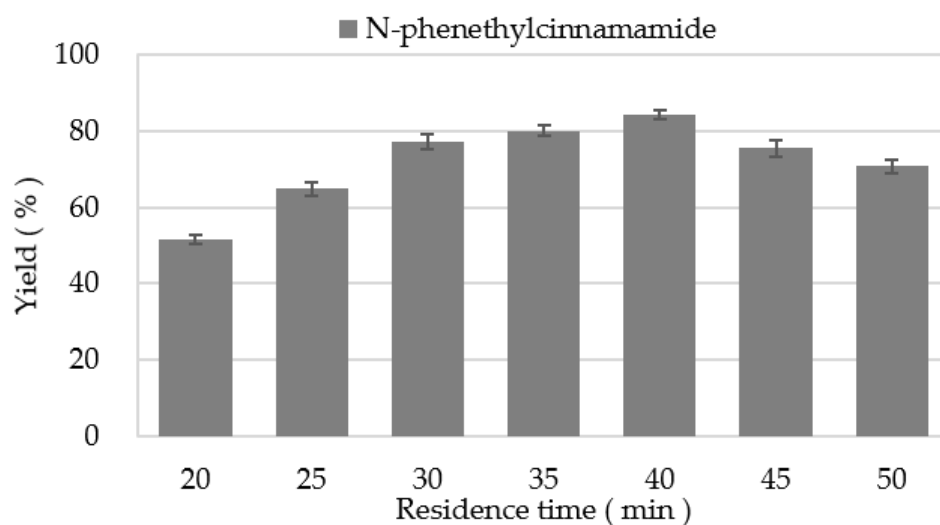


**Figure 4.** The effect of residence time on the synthesis of N-phenethylcinnamamide catalyzed by Lipozyme<sup>®</sup> TL IM in continuous-flow microreactors.

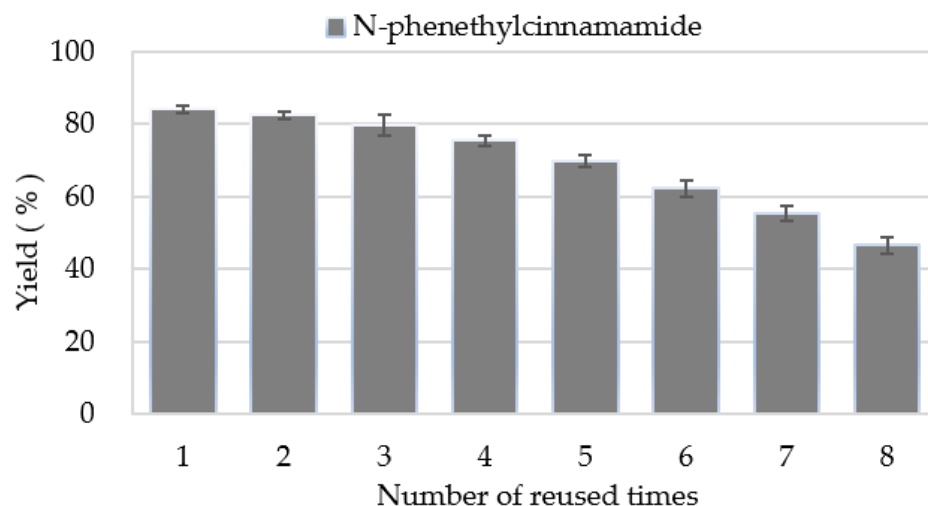


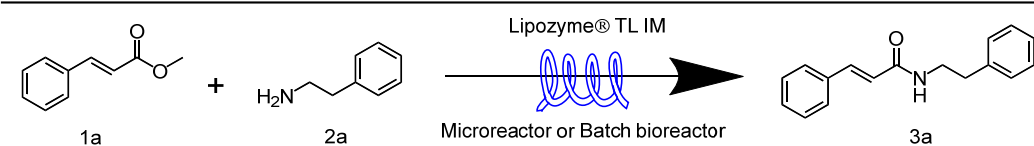
**Figure 5.** The effect of reused times on the synthesis of N-phenethylcinnamamide catalyzed by Lipozyme<sup>®</sup> TL IM in continuous-flow microreactors.

### 2.6. Comparing the Synthesis of Cinnamamide Derivatives from Methyl Cinnamates and Phenylethylamines in a Continuous-Flow Microreactor and a Batch Bioreactor

To investigate the effect of enzymatic reactions in different reactors, we optimized the conditions of enzymatic reactions in a continuous-flow microreactor and a batch bioreactor for the synthesis of N-phenethylcinnamamide. (Table 2) In the batch bioreactor (method B), it took about 24 h to reach the expected yield. However, in the continuous-flow microreactor, better yields were obtained in 40 min (method A). Space-time yield (STY) is a common index to evaluate the production capacity of different reactors [56–60]. Therefore, we calculated STY(g L<sup>-1</sup> h<sup>-1</sup>) to evaluate the productivity in the two reactors and found that the STY in the continuous-flow microreactor was higher. The results suggest that the choice of continuous-flow microreactors is more favorable to improve the efficiency of enzymatic synthesis of cinnamamide derivatives.

$$STY = m_p \times T^{-1} \times V_R^{-1} \quad (1)$$

where  $m_p$  is the mass of the generated product (g),  $T$  is the residence time (h), and  $V_R$  is the reactor volume (L).

**Table 2.** Enzyme-catalyzed synthesis of N-phenethylcinnamamide in a Continuous-Flow Microreactor or a Batch Bioreactor <sup>a</sup>.


The reaction scheme shows methyl cinnamate (1a) reacting with phenylethylamine (2a) in the presence of the enzyme Lipozyme® TL IM, catalyzed in either a microreactor or a batch bioreactor, to produce N-phenethylcinnamamide (3a).

Entry	Method	STY (g L <sup>-1</sup> h <sup>-1</sup> )	Yield <sup>b</sup> (%)
1	A	20.68	84.2 ± 1.2
2	B	1.09	64.3 ± 0.8

<sup>a</sup> Reaction conditions: Method A: feed 1, 5.0 mmol methyl cinnamate (1a) dissolved in 10 mL *tert*-amyl alcohol, feed 2, 10.0 mmol phenylethylamine (2a) dissolved in 10 mL *tert*-amyl alcohol, Lipozyme® TL IM (catalyst reactivity: 250IUN·g<sup>-1</sup>) 0.87 g, flow rate 15.6 μL min<sup>-1</sup>, 40 min residence time at 45 °C. Method B: batch bioreactor, 5.0 mmol methyl cinnamate (1a), and 10.0 mmol phenylethylamine added to 20 mL *tert*-amyl alcohol, Lipozyme® TL IM (catalyst reactivity: 250IUN·g<sup>-1</sup>) 0.87 g, 200 r min<sup>-1</sup>, 45 °C, 24 h. <sup>b</sup> Isolated yield. Yield: 100× (actual received quality/ideal calculated quality). The data are presented as average ± SD of triplicate experiments.

### 2.7. The Scope and Limitation of the Synthesis of Cinnamamide Derivatives Catalyzed by Lipozyme® TL IM in Continuous-Flow Microreactors

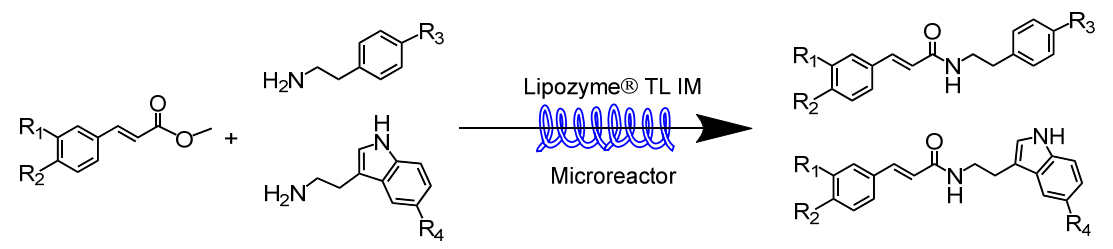
In the ammonolysis of esters, ammonia can attach to the α-carbon in the carbonyl group of the ester as a nucleophile. The electronic part on the α-carbon is transferred to oxygen, and then the amine cation can provide a proton to the methoxy group to generate methanol leaving the group, thus forming an amide [26]. We further studied the scope and limitations of the enzymatic aminolysis of cinnamate derivatives under continuous-flow microreactors; the reactions of four methyl cinnamate derivatives (methyl cinnamate, methyl *trans*-p-Coumarate, methyl ferulate, and methyl 4-chlorocinnamate) with four amine compounds (phenylethylamine, tyramine, tryptamine, and 5-methoxytryptamine) were studied under optimal reaction conditions (40 min, 45 °C, *tert*-amyl alcohol, methyl cinnamate derivative:amine compound = 1:2) in continuous-flow microreactors. As shown in Table 3, we found that the substituents on the benzene ring of the ester would affect the reactivity of the ammonolysis reaction. When there was an electron withdrawing on the benzene ring, it was conducive to the reaction, and when there was an electron-donating group, it reduced the reactivity. Then, we studied the effects of different amine compounds on the reaction and found that the substituents on the benzene ring or indole ring had no significant effect on the reaction, which may be due to the fact that phenylethylamines had a long fat chain and weakened the influence of substituents.

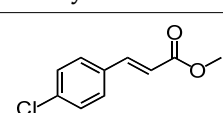
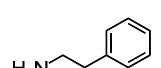
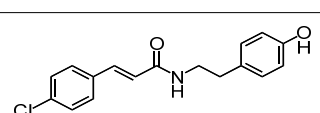
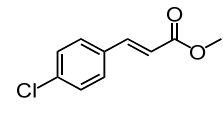
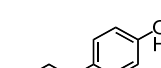
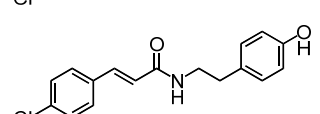
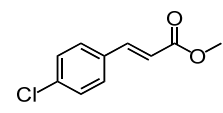
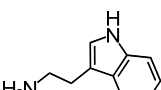
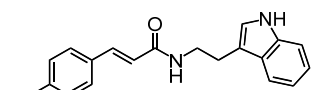
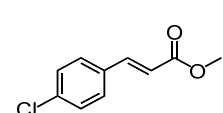
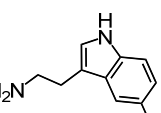
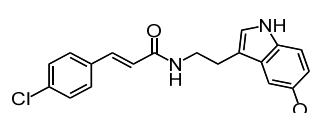
**Table 3.** Effect of substrate structure on the synthesis of cinnamamide derivatives catalyzed by Lipozyme® TL IM in continuous-flow microreactors <sup>a</sup>.

Entry	Methyl Cinnamates	Amine Compounds	Product	Yield <sup>b</sup> (%)
1				84.2 ± 1.2
2				80.4 ± 0.8
3				60.2 ± 0.7
4				55.2 ± 1.3
5				72.8 ± 0.9
6				67.9 ± 0.6
7				54.4 ± 1.2
8				49.8 ± 0.9
9				62.5 ± 2.4
10				54.5 ± 1.6
11				44.9 ± 0.9
12				44.4 ± 0.8



Table 3. Cont.



Entry	Methyl Cinnamates	Amine Compounds	Product	Yield <sup>b</sup> (%)
13				91.3 ± 1.3
14				85.3 ± 1.1
15				67.6 ± 0.7
16				62.6 ± 1.8

<sup>a</sup> Reaction conditions: feed 1, 5.0 mmol methyl cinnamate derivative dissolved in 10 mL *tert*-amyl alcohol, feed 2, 10.0 mmol amine compounds dissolved in 10 mL *tert*-amyl alcohol, Lipozyme<sup>®</sup> TL IM (catalyst reactivity: 250 IUN·g<sup>-1</sup>) 0.87 g, flow rate 15.6 μL min<sup>-1</sup>, 40 min residence time at 45 °C. <sup>b</sup> Isolated yield. Yield: 100 × (actual received quantity/ideal calculated quantity). The data are presented as average ± SD of triplicate experiments.

### 3. Materials and Methods

#### 3.1. Materials

All chemicals in this study were obtained from commercial sources and did not require further purification. Subtilisin<sup>®</sup> was purchased from Sigma., and Lipozyme<sup>®</sup> TL IM from *Thermomyces lanuginosus* was purchased from Novo Nordisk (Copenhagen, Denmark). Methyl cinnamate, 5-methoxytryptamine was purchased from Shanghai bide Pharmaceutical Technology Co., Ltd. (Shanghai, China). Methyl *trans-p*-Coumarate, tyramine was obtained from Aladdin (Shanghai, China). Methyl ferulat, phenylethylamine was obtained from Innochem (Beijing, China). Methyl 4-chlorocinnamate was purchased from Macklin (Shanghai, China). Tryptamine was purchased from Rhawn (Shanghai, China). Harvard Instrument PHD 2000 syringe pump was purchased from Harvard University (Holliston, MA, USA). The flow reactor and Y-mixer were purchased from Beijing Haigui Medical Engineering Design Co., Ltd. (Beijing, China). A 400 MHz NMR spectrometer (Billerica, MA, USA) was also used in this study.

#### 3.2. Experimental Setup and Experiment Conditions

The apparatus configuration used for the synthesis of cinnamamide derivatives in the continuous-flow microreactor is shown in Figure 6 and Figure S1. The experimental setup consisted of five main parts: a syringe pump (Harvard Apparatus Dr. 2000), substrate injectors, a Y-mixer, a flow reactor, and a product collector. Preparation: the flow reactor (2 mm inner diameter) was first filled with 0.87 g Lipozyme<sup>®</sup> TL IM with a particle size of 0.3–1.0 mm, reactivity of 250 IUN·g<sup>-1</sup>, followed by immersing the reactor in a constant temperature water bath at 45 °C. Starting of work: 5.0 mmol methyl cinnamate derivative dissolved in 10 mL *tert*-amyl alcohol in feed 1 and 10.0 mmol amine dissolved in 10 mL

*tert*-amyl alcohol in feed 2. The two solutions were intersected in the Y-mixer, and the mixed stream was passed through the flow reactor at a flow rate of  $15.6 \mu\text{L min}^{-1}$  with a residence time of 40 min. The reaction solution was finally collected, evaporated, and dried. Following up: The products were separated by silica gel chromatography (eluent: petroleum ether/ethyl acetate from 10/1 to 2/1). The main products were determined by  $^1\text{H}$  NMR and  $^{13}\text{C}$  NMR.

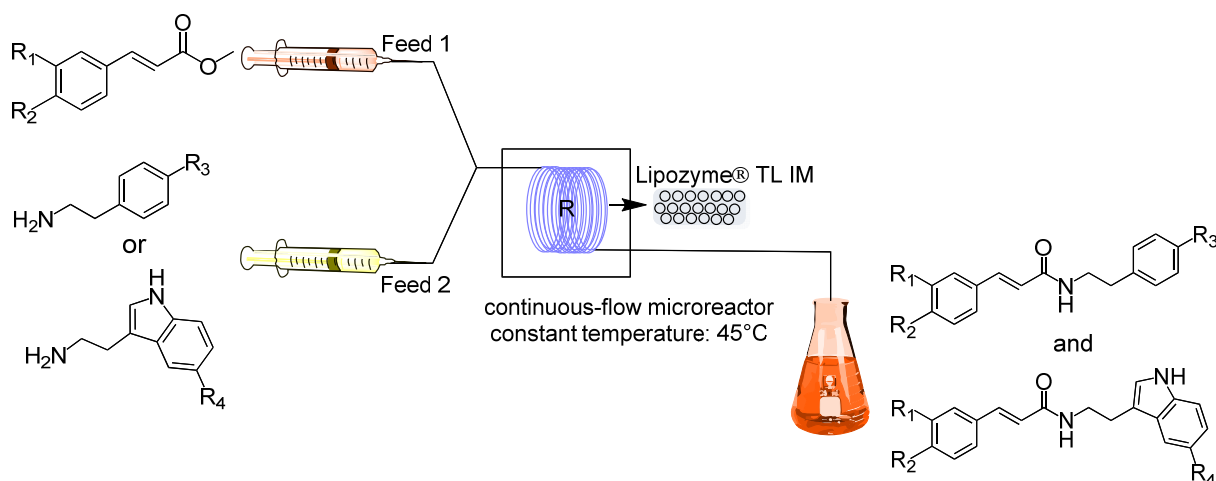


**Figure 6.** Equipment for the synthesis of cinnamamides from methyl cinnamates and phenylethylenamines catalyzed by Lipozyme® TL IM under continuous-flow microreactors.

### 3.3. Analytical Methods

#### 3.3.1. Thin-Layer Chromatography (TLC)

The developing solvent was petroleum ether/ethyl acetate from 6/1 (*v/v*) to 1/1 (*v/v*), and the results are detected under UV light irradiation at 254 nm.

#### 3.3.2. Nuclear Magnetic Resonance (NMR)

The product obtained by column chromatography separation and purification was subjected to  $^1\text{H}$  NMR and  $^{13}\text{C}$  NMR structure confirmation on NMR spectrometer.

*N*-phenethylcinnamamide (3a). White powder.  $^1\text{H}$  NMR (400 MHz,  $\text{DMSO-}d_6$ )  $\delta$  8.21 (t,  $J = 5.6$  Hz, 1H), 7.57–7.50 (m, 2H), 7.43–7.14 (m, 9H), 6.59 (d,  $J = 15.9$  Hz, 1H), 3.40–3.27 (m, 2H), 2.76 (t,  $J = 7.3$  Hz, 2H).;  $^{13}\text{C}$  NMR (101 MHz,  $\text{DMSO}$ )  $\delta$  165.16, 139.62, 138.82, 135.04, 129.66, 129.14, 128.84, 128.56, 127.71, 126.33, 122.31, 40.56, 35.30.

*N*-(4-hydroxyphenethyl)cinnamamide (3b). White powder.  $^1\text{H}$  NMR (500 MHz,  $\text{DMSO-}d_6$ )  $\delta$  9.19 (s, 1H), 8.15 (t,  $J = 5.7$  Hz, 1H), 7.55 (d,  $J = 7.4$  Hz, 2H), 7.45–7.34 (m, 4H), 7.02 (d,  $J = 8.2$  Hz, 2H), 6.72–6.65 (m, 2H), 6.62 (d,  $J = 15.8$  Hz, 1H), 3.34–3.32 (m, 2H), 2.66 (t,  $J = 7.5$  Hz, 2H).;  $^{13}\text{C}$  NMR (101 MHz,  $\text{DMSO}$ )  $\delta$ : 165.06, 155.77, 138.65, 135.06, 129.60, 129.58, 129.46, 128.99, 127.58, 122.43, 115.27, 40.86, 34.48.

*N*-(2-(1*H*-indol-3-yl)ethyl)cinnamamide (3c). Orange yellow solid.  $^1\text{H}$  NMR (400 MHz,  $\text{DMSO-}d_6$ )  $\delta$  10.81–10.77 (m, 1H), 8.20 (t,  $J = 5.7$  Hz, 1H), 7.55–7.49 (m, 3H), 7.44–7.27 (m, 5H), 7.13 (d,  $J = 2.3$  Hz, 1H), 7.03 (ddd,  $J = 8.1, 6.9, 1.2$  Hz, 1H), 6.94 (ddd,  $J = 8.0, 6.9, 1.1$  Hz, 1H), 6.60 (d,  $J = 15.8$  Hz, 1H), 3.44 (td,  $J = 7.4, 5.7$  Hz, 2H), 2.85 (t,  $J = 7.4$  Hz, 2H).;  $^{13}\text{C}$  NMR (101 MHz,  $\text{DMSO}$ )  $\delta$  165.01, 138.57, 136.36, 135.07, 129.50, 129.05, 127.60, 127.33, 122.79, 122.49, 121.05, 118.39, 118.35, 111.88, 111.49, 39.73, 25.35.

*N*-(2-(5-methoxy-1*H*-indol-3-yl)ethyl)cinnamamide (3d). Yellow powder.  $^1\text{H}$  NMR (400 MHz,  $\text{DMSO-}d_6$ )  $\delta$  10.66 (s, 1H), 8.23 (q,  $J = 4.8, 4.2$  Hz, 1H), 7.55 (ddd,  $J = 8.1, 3.4, 1.7$  Hz, 2H), 7.48–7.34 (m, 4H), 7.25–7.19 (m, 1H), 7.13 (d,  $J = 2.5$  Hz, 1H), 7.04 (d,  $J = 2.5$  Hz, 1H), 6.74–6.68 (m, 1H), 6.68–6.60 (m, 1H), 3.76–3.72 (m, 3H), 3.46 (td,  $J = 7.5, 4.2$  Hz, 2H), 2.85 (td,  $J = 7.3, 2.5$  Hz, 2H).;  $^{13}\text{C}$  NMR (101 MHz,  $\text{DMSO}$ )  $\delta$  165.01, 153.08, 138.56, 135.07, 131.49, 129.50, 129.05, 127.67, 127.59, 123.47, 122.52, 112.13, 111.75, 111.21, 100.20, 55.39, 40.51, 25.35.

(*E*)-3-(4-hydroxyphenyl)-*N*-phenethylacrylamide (3e). White powder.  $^1\text{H}$  NMR (400 MHz,  $\text{DMSO-}d_6$ )  $\delta$  9.88 (s, 1H), 8.07 (t,  $J = 5.7$  Hz, 1H), 7.34 (dd,  $J = 24.1, 8.6$  Hz, 3H), 7.28–7.17 (m, 5H), 6.80–6.73 (m, 2H), 6.37 (dd,  $J = 15.8, 1.1$  Hz, 1H), 3.40–3.33 (m, 2H), 2.75 (t,  $J = 7.4$  Hz, 2H).;  $^{13}\text{C}$  NMR (101 MHz,  $\text{DMSO-}d_6$ )  $\delta$  165.64, 159.00, 139.69, 138.92, 129.43, 128.83, 128.55, 126.30, 126.06, 118.76, 115.93, 40.53, 35.38.

(*E*)-*N*-(4-hydroxyphenethyl)-3-(4-hydroxyphenyl)acrylamide (3f). White powder.  $^1\text{H}$  NMR (400 MHz,  $\text{DMSO-}d_6$ )  $\delta$  9.81 (s, 1H), 9.15 (s, 1H), 7.99 (t,  $J = 5.7$  Hz, 1H), 7.40–7.34 (m, 2H), 7.30 (d,  $J = 15.7$  Hz, 1H), 7.04–6.97 (m, 2H), 6.81–6.74 (m, 2H), 6.71–6.63 (m, 2H), 6.38 (d,  $J = 15.7$  Hz, 1H), 3.32–3.28 (m, 2H), 2.63 (t,  $J = 7.4$  Hz, 2H).;  $^{13}\text{C}$  NMR (101 MHz,  $\text{DMSO}$ )  $\delta$  165.37, 158.86, 155.70, 138.63, 129.62, 129.55, 129.25, 126.01, 118.83, 115.81, 115.19, 40.75, 34.52.

(*E*)-*N*-(2-(1*H*-indol-3-yl)ethyl)-3-(4-hydroxyphenyl)acrylamide (3g). Orange yellow solid.  $^1\text{H}$  NMR (400 MHz,  $\text{DMSO-}d_6$ )  $\delta$  10.80 (d,  $J = 2.6$  Hz, 1H), 9.82 (s, 1H), 8.08 (t,  $J = 5.8$  Hz, 1H), 7.54 (dd,  $J = 7.7, 1.1$  Hz, 1H), 7.40–7.28 (m, 4H), 7.15 (d,  $J = 2.4$  Hz, 1H), 7.05 (ddd,  $J = 8.1, 6.9, 1.2$  Hz, 1H), 6.96 (ddd,  $J = 8.0, 7.0, 1.1$  Hz, 1H), 6.81–6.74 (m, 2H), 6.40 (d,  $J = 15.8$  Hz, 1H), 3.49–3.39 (m, 2H), 2.86 (t,  $J = 7.4$  Hz, 2H).;  $^{13}\text{C}$  NMR (101 MHz,  $\text{DMSO}$ )  $\delta$  165.47, 158.89, 138.67, 136.36, 129.30, 127.34, 126.06, 122.76, 121.04, 118.93, 118.40, 118.34, 115.85, 111.95, 111.48, 39.67, 25.43.

(*E*)-3-(4-hydroxyphenyl)-*N*-(2-(5-methoxy-1*H*-indol-3-yl)ethyl)acrylamide (3h). Yellow solid.  $^1\text{H}$  NMR (400 MHz,  $\text{DMSO-}d_6$ )  $\delta$  10.64–10.60 (m, 1H), 9.81 (s, 1H), 8.06 (t,  $J = 5.8$  Hz, 1H), 7.38–7.30 (m, 2H), 7.28 (s, 1H), 7.19 (d,  $J = 8.8$  Hz, 1H), 7.09 (d,  $J = 2.4$  Hz, 1H), 7.00 (d,  $J = 2.4$  Hz, 1H), 6.79–6.72 (m, 2H), 6.67 (dd,  $J = 8.7, 2.4$  Hz, 1H), 6.38 (d,  $J = 15.8$  Hz, 1H), 3.71 (s, 3H), 3.39 (dd,  $J = 14.3, 7.6$  Hz, 2H), 2.81 (t,  $J = 7.3$  Hz, 2H).;  $^{13}\text{C}$  NMR (101 MHz,  $\text{DMSO}$ )  $\delta$  165.47, 158.87, 153.06, 138.64, 131.47, 129.27, 127.67, 126.06, 123.43, 118.96, 115.84, 112.10, 111.80, 111.19, 100.21, 55.39, 48.71, 25.42.

(*E*)-3-(4-hydroxy-3-methoxyphenyl)-*N*-phenethylacrylamide (3i). White solid.  $^1\text{H}$  NMR (400 MHz,  $\text{DMSO-}d_6$ )  $\delta$  9.47 (s, 1H), 8.08 (t,  $J = 5.7$  Hz, 1H), 7.37 (d,  $J = 15.7$  Hz, 1H), 7.33–7.16 (m, 5H), 7.14 (d,  $J = 2.0$  Hz, 1H), 7.01 (dd,  $J = 8.2, 2.0$  Hz, 1H), 6.82 (d,  $J = 8.1$  Hz, 1H), 6.48 (d,  $J = 15.7$  Hz, 1H), 3.81 (s, 3H), 3.47–3.40 (m, 2H), 2.79 (t,  $J = 7.3$  Hz, 2H).;  $^{13}\text{C}$  NMR (101 MHz,  $\text{DMSO}$ )  $\delta$  165.62, 148.43, 147.98, 139.66, 139.19, 128.78, 128.48, 126.58, 126.23, 121.72, 119.09, 115.82, 110.90, 55.65, 40.49, 35.38.

(*E*)-3-(4-hydroxy-3-methoxyphenyl)-*N*-(4-hydroxyphenethyl)acrylamide (3j). White powder.  $^1\text{H}$  NMR (500 MHz,  $\text{DMSO-}d_6$ )  $\delta$  9.37 (s, 1H), 9.13 (s, 1H), 7.94 (t,  $J = 5.7$  Hz, 1H), 7.26 (d,  $J = 15.7$  Hz, 1H), 7.07 (d,  $J = 2.0$  Hz, 1H), 7.00–6.94 (m, 2H), 6.94 (dd,  $J = 8.2, 2.0$  Hz, 1H), 6.74 (d,  $J = 8.1$  Hz, 1H), 6.68–6.60 (m, 2H), 6.38 (d,  $J = 15.7$  Hz, 1H), 3.76 (s, 3H), 3.28 (s, 2H), 2.60 (t,  $J = 7.4$  Hz, 2H).;  $^{13}\text{C}$  NMR (101 MHz,  $\text{DMSO}$ )  $\delta$ : 165.85, 156.08, 148.72, 148.31, 139.37, 130.02, 129.92, 126.94, 121.99, 119.53, 116.15, 115.60, 111.31, 56.04, 41.12, 34.88.

(*E*)-*N*-(2-(1*H*-indol-3-yl)ethyl)-3-(4-hydroxy-3-methoxyphenyl)acrylamide (3k). Orange solid.  $^1\text{H}$  NMR (400 MHz,  $\text{DMSO-}d_6$ )  $\delta$  10.85–10.80 (m, 1H), 9.44 (s, 1H), 8.07 (t,  $J = 5.7$  Hz, 1H), 7.56 (d,  $J = 7.8$  Hz, 1H), 7.44–7.23 (m, 2H), 7.42–6.94 (m, 5H), 6.79 (d,  $J = 8.1$  Hz, 1H), 6.45 (d,  $J = 15.7$  Hz, 1H), 3.80 (s, 3H), 3.52–3.42 (m, 2H), 2.88 (t,  $J = 7.4$  Hz, 2H).;  $^{13}\text{C}$  NMR (101 MHz,  $\text{DMSO}$ )  $\delta$  165.44, 148.31, 147.91, 138.95, 136.35, 127.33, 126.54, 122.75, 121.60, 121.03, 119.22, 118.38, 118.33, 115.73, 111.92, 111.47, 110.80, 55.60, 40.01, 25.40.

(*E*)-3-(4-hydroxy-3-methoxyphenyl)-*N*-(2-(5-methoxy-1*H*-indol-3-yl)ethyl)acrylamide (3l). Orange solid.  $^1\text{H}$  NMR (400 MHz,  $\text{DMSO-}d_6$ )  $\delta$  10.64–10.60 (m, 1H), 9.40 (s, 1H), 8.04 (t,  $J = 5.7$  Hz, 1H), 7.30 (d,  $J = 15.6$  Hz, 1H), 7.19 (d,  $J = 8.8$  Hz, 1H), 7.08 (t,  $J = 2.7$  Hz, 2H), 7.03–6.92 (m, 2H), 6.75 (d,  $J = 8.1$  Hz, 1H), 6.67 (dd,  $J = 8.7, 2.4$  Hz, 1H), 6.42 (d,  $J = 15.7$  Hz, 1H), 3.76 (s, 3H), 3.71 (s, 3H), 3.41 (q,  $J = 6.8$  Hz, 2H), 2.81 (t,  $J = 7.3$  Hz, 2H).;  $^{13}\text{C}$  NMR (101 MHz,  $\text{DMSO}$ )  $\delta$  165.48, 153.07, 148.31, 147.92, 138.94, 131.49, 127.69, 126.56, 123.44, 121.58, 119.26, 115.75, 112.11, 111.80, 111.19, 110.82, 100.23, 55.62, 55.41, 48.72, 25.42.

(*E*)-3-(4-chlorophenyl)-*N*-phenethylacrylamide (3m). White solid,  $^1\text{H}$  NMR (400 MHz,  $\text{DMSO-}d_6$ )  $\delta$  8.18 (t,  $J = 5.7$  Hz, 1H), 7.58–7.51 (m, 2H), 7.46–7.41 (m, 2H), 7.36 (d,  $J = 15.8$  Hz, 1H), 7.30–7.13 (m, 5H), 6.58 (d,  $J = 15.8$  Hz, 1H), 3.42–3.34 (m, 2H), 2.74 (t,  $J = 7.3$  Hz, 2H).;  $^{13}\text{C}$  NMR (101 MHz,  $\text{DMSO}$ )  $\delta$  164.82, 139.53, 137.33, 133.99, 133.93, 129.33, 129.08, 128.75, 128.47, 126.24, 123.12, 40.47, 35.21.

(*E*)-3-(4-chlorophenyl)-*N*-(4-hydroxyphenethyl)acrylamide (3n). White powder.  $^1\text{H}$  NMR (400 MHz,  $\text{DMSO-}d_6$ )  $\delta$  9.18 (s, 1H), 8.16 (t,  $J = 5.7$  Hz, 1H), 7.60–7.53 (m, 2H), 7.50–7.42 (m, 2H), 7.38 (d,  $J = 15.8$  Hz, 1H), 7.04–6.97 (m, 2H), 6.71–6.63 (m, 2H), 6.61 (d,  $J = 15.8$  Hz, 1H), 3.36 (s, 2H), 2.64 (t,  $J = 7.4$  Hz, 2H).;  $^{13}\text{C}$  NMR (101 MHz,  $\text{DMSO}$ )  $\delta$  164.75, 155.76, 137.25, 134.01, 133.91, 129.60, 129.54, 129.32, 129.07, 123.19, 115.23, 40.83, 34.43.

(*E*)-*N*-(2-(1*H*-indol-3-yl)ethyl)-3-(4-chlorophenyl)acrylamide (3o). Yellow solid.  $^1\text{H}$  NMR (400 MHz,  $\text{DMSO-}d_6$ )  $\delta$  10.83–10.77 (m, 1H), 8.22 (t,  $J = 5.8$  Hz, 1H), 7.55 (dd,  $J = 11.4$ , 8.2 Hz, 3H), 7.49–7.44 (m, 2H), 7.40 (d,  $J = 15.8$  Hz, 1H), 7.32 (d,  $J = 8.1$  Hz, 1H), 7.15 (d,  $J = 2.3$  Hz, 1H), 7.05 (ddd,  $J = 8.1$ , 6.9, 1.2 Hz, 1H), 6.96 (ddd,  $J = 7.9$ , 7.0, 1.1 Hz, 1H), 6.62 (d,  $J = 15.8$  Hz, 1H), 3.50–3.41 (m, 2H), 2.87 (t,  $J = 7.3$  Hz, 2H).;  $^{13}\text{C}$  NMR (101 MHz,  $\text{DMSO}$ )  $\delta$  164.77, 137.20, 136.34, 134.04, 133.87, 129.28, 129.05, 127.30, 123.30, 122.77, 121.02, 118.36, 118.33, 111.83, 111.46, 39.71, 25.29.

(*E*)-3-(4-chlorophenyl)-*N*-(2-(5-methoxy-1*H*-indol-3-yl)ethyl)acrylamide (3p). Yellow powder.  $^1\text{H}$  NMR (400 MHz,  $\text{DMSO-}d_6$ )  $\delta$  10.62 (d,  $J = 2.3$  Hz, 1H), 8.21 (t,  $J = 5.8$  Hz, 1H), 7.58–7.51 (m, 2H), 7.48–7.42 (m, 2H), 7.39 (d,  $J = 15.8$  Hz, 1H), 7.19 (d,  $J = 8.7$  Hz, 1H), 7.09 (d,  $J = 2.3$  Hz, 1H), 7.00 (d,  $J = 2.4$  Hz, 1H), 6.67 (dd,  $J = 8.7$ , 2.4 Hz, 1H), 6.61 (d,  $J = 15.9$  Hz, 1H), 3.71 (s, 3H), 3.43 (q,  $J = 6.8$  Hz, 2H), 2.82 (t,  $J = 7.3$  Hz, 2H).;  $^{13}\text{C}$  NMR (101 MHz,  $\text{DMSO}$ )  $\delta$  164.81, 153.08, 137.21, 134.04, 133.89, 131.49, 129.29, 129.07, 127.66, 123.46, 123.32, 112.12, 111.71, 111.20, 100.22, 55.40, 40.02, 25.31.

#### 4. Conclusions

In conclusion, the highly efficient synthesis of cinnamamides from methyl cinnamates and phenylethylamines catalyzed by Lipozyme<sup>®</sup> TL IM under continuous-flow microreactors was developed. Lipozyme<sup>®</sup> TL IM was first used for the synthetic reaction of cinnamamides from methyl cinnamates and phenylethylamines by ammonolysis reaction. Combined with the specificity of enzyme catalysis and the efficiency of continuous-flow technology, the effects of reaction solvent, reaction temperature, reaction substrate ratio, reaction residence time, and reactant structure on the synthesis of cinnamamides were studied. The remarkable features of this study include short residence time (40 min), mild temperature (45 °C), environmental protection of catalysts, and easy control of the reaction process. Next, we will delve into more syntheses of cinnamamides, such as different amines, and explore more efficient and green synthesis methods for cinnamide derivatives. The synthesized cinnamide structures can be introduced into drug molecules to prepare new composite drugs, thus laying a broader scope for drug screening.

**Supplementary Materials:** The following supporting information can be downloaded at: <https://www.mdpi.com/article/10.3390/catal12101265/s1>, Figure S1: Equipment for the synthesis of cinnamamides from methyl cinnamates and phenylethylamines catalyzed by Lipozyme<sup>®</sup> TL IM under continuous-flow microreactors. References [7,19,61–66] are cited in the Supplementary Materials.

**Author Contributions:** L.Z. and L.D. subject selection, experimental design, and drafted and revised the manuscript; L.Z. and Y.P. background research and experimental optimization; Z.S., S.Z., H.L., A.Z. and H.X. collected data; L.Z., L.D. and X.L. analyzed the data and revised the manuscript. All authors have read and agreed to the published version of the manuscript.

**Funding:** This research was funded by the Natural Science Foundation of Zhejiang Province grant number (LGN20C200020 and KYHX-20211096), the Key Research & Development Projects of Zhejiang Province grant number (2020C03090), the Zhejiang Provincial Key Discipline of Chemistry Biology, the National Science and Technology Support Project (2015BAD14B0305), the National Natural Science Foundation of China (21306172), and the Science and Technology Research Program of Zhejiang Province grant number (2014C32094), and the APC was funded by the Natural Science Foundation of Zhejiang University of Technology grant number (116004029).

**Data Availability Statement:** Not applicable.

**Acknowledgments:** We thank the Natural Science Foundation of Zhejiang Province and the Key Research and Development Projects of Zhejiang Province (LGN20C200020 and 2020C03090 and KYYHX-20211096), the Zhejiang Provincial Key Discipline of Chemistry Biology, the National Science and Technology Support Project (2015BAD14B0305), the National Natural Science Foundation of China (21306172), and the Science and Technology Research Program of Zhejiang Province (2014C32094), as well as the Natural Science Foundation of Zhejiang University of Technology (116004029) for financial support.

**Conflicts of Interest:** The authors declare no conflict of interest.

## References

1. Gaspar, A.; Garrido, E.M.; Esteves, M.E.; Quezada, E.; Milhazes, N.; Garrido, J.; Borges, F. New insights into the antioxidant activity of hydroxycinnamic acids: Synthesis and physicochemical characterization of novel halogenated derivatives. *Eur. J. Med. Chem.* **2009**, *44*, 2092–2099. [[CrossRef](#)] [[PubMed](#)]
2. Guzman, J.D. Natural cinnamic acids, synthetic derivatives and hybrids with antimicrobial activity. *Molecules* **2014**, *19*, 19292–19349. [[CrossRef](#)] [[PubMed](#)]
3. De, P.; Baltas, M.; Bedos-Belval, F. Cinnamic Acid Derivatives as Anticancer Agents—A Review. *Curr. Med. Chem.* **2011**, *18*, 1672–1703. [[CrossRef](#)] [[PubMed](#)]
4. Liao, J.C.; Deng, J.S.; Chiu, C.S.; Hou, W.C.; Huang, S.S.; Shie, P.H.; Huang, G.J. Anti-Inflammatory Activities of *Cinnamomum cassia* Constituents In Vitro and In Vivo. *Evid. Based Complement. Altern. Med.* **2012**, *2012*, 429320. [[CrossRef](#)]
5. Chen, D.D.; Zhang, B.Y.; Liu, X.X.; Li, X.Q.; Yang, X.J.; Zhou, L. Bioactivity and structure-activity relationship of cinnamic acid derivatives and its heteroaromatic ring analogues as potential high-efficient acaricides against *Psoroptes cuniculi*. *Bioorganic Med. Chem. Lett.* **2018**, *28*, 1149–1153. [[CrossRef](#)]
6. Chen, G.Z.; Zhang, Y.L.; Liu, X.; Fang, Q.L.; Wang, Z.; Fu, L.L.; Liu, Z.G.; Wang, Y.; Zhao, Y.J.; Li, X.K.; et al. Discovery of a New Inhibitor of Myeloid Differentiation 2 from Cinnamamide Derivatives with Anti-Inflammatory Activity in Sepsis and Acute Lung Injury. *J. Med. Chem.* **2016**, *59*, 2436–2451. [[CrossRef](#)]
7. Chan, H.H.; Hwang, T.L.; Thang, T.D.; Leu, Y.L.; Kuo, P.C.; Nguyet, B.T.M.; Dai, D.N.; Wu, T.S. Isolation and synthesis of melodamide A, a new anti-inflammatory phenolic amide from the leaves of *Melodorum fruticosum*. *Planta Med.* **2013**, *79*, 288–294. [[CrossRef](#)]
8. He, F.C.; Chou, J.; Scheiner, M.; Poeta, E.; Chen, N.Y.; Gunesch, S.; Hoffmann, M.; Sottriffer, C.; Monti, B.; Maurice, T.; et al. Melatonin- and Ferulic Acid-Based HDAC6 Selective Inhibitors Exhibit Pronounced Immunomodulatory Effects In Vitro and Neuroprotective Effects in a Pharmacological Alzheimer’s Disease Mouse Model. *J. Med. Chem.* **2021**, *64*, 3794–3812. [[CrossRef](#)]
9. Chen, L.; Zhang, J.L.; Zhao, B.; Fan, Z.J.; Hu, M.X.; Li, Q.; Hu, W.H.; Li, J.W. Discovery of Novel Isothiazole, 1,2,3-Thiadiazole, and Thiazole-Based Cinnamamides as Fungicidal Candidates. *J. Agric. Food Chem.* **2019**, *67*, 12357–12365. [[CrossRef](#)]
10. Wang, D.; Zhu, J.; Xu, J.R.; Ji, D.D. Synthesis of N-hydroxycinnamoyl amide derivatives and evaluation of their anti-oxidative and anti-tyrosinase activities. *Bioorganic Med. Chem.* **2019**, *27*, 114918. [[CrossRef](#)]
11. Kim, J.K.; Heo, H.Y.; Park, S.; Kim, H.; Oh, J.J.; Sohn, E.H.; Jung, S.H.; Lee, K. Characterization of Phenethyl Cinnamamide Compounds from Hemp Seed and Determination of Their Melanogenesis Inhibitory Activity. *ACS Omega* **2021**, *6*, 31945–31954. [[CrossRef](#)] [[PubMed](#)]
12. Yang, Y.; Song, G.Z.; Liu, Z.Q. Synthesis and antioxidant capacities of hydroxyl derivatives of cinnamoylphenethylamine in protecting DNA and scavenging radicals. *Free Radic. Res.* **2011**, *45*, 445–453. [[CrossRef](#)]
13. Han, E.H.; Kim, J.Y.; Kim, H.G.; Choi, J.H.; Im, J.H.; Woo, E.R.; Jeong, H.G. Dihydro-N-caffeoyltyramine down-regulates cyclooxygenase-2 expression by inhibiting the activities of C/EBP and AP-1 transcription factors. *Food Chem. Toxicol.* **2010**, *48*, 579–586. [[CrossRef](#)] [[PubMed](#)]
14. Song, Y.H.; Kim, D.W.; Long, M.J.; Park, C.; Son, M.; Kim, J.K.; Yuk, H.J.; Lee, K.W.; Park, K.H. Cinnamic acid amides from *Tribulus terrestris* displaying uncompetitive  $\alpha$ -glucosidase inhibition. *Eur. J. Med. Chem.* **2016**, *114*, 201–208. [[CrossRef](#)]
15. Thomas, J.B.; Fall, M.J.; Cooper, J.B.; Burgess, J.P.; Carroll, F.I. Rapid In-Plate Generation of Benzimidazole Libraries and Amide Formation Using EEDQ. *Tetrahedron Lett.* **1997**, *38*, 5099–5102. [[CrossRef](#)]
16. Kunishima, M.; Kawachi, C.; Morita, J.; Terao, K.; Iwasaki, F.; Tani, S. 4-(4,6-Dimethoxy-1,3,5-triazin-2-yl)-4-methylmorpholinium Chloride: An Efficient Condensing Agent Leading to the Formation of Amides and Esters. *Tetrahedron* **1999**, *55*, 13159–13170. [[CrossRef](#)]
17. Garrett, C.E.; Jiang, X.L.; Prasad, K.; Repič, O. New observations on peptide bond formation using CDMT. *Tetrahedron Lett.* **2002**, *43*, 4161–4165. [[CrossRef](#)]
18. Hioki, K.; Kameyama, S.; Tani, S.; Kunishima, M. Immobilized Triazine-Type Dehydrocondensing Reagents for Carboxamide Formation: ROMP-Trz-Cl and ROMP(OH)-Trz-Cl. *Chem. Pharm. Bull.* **2007**, *55*, 825–828. [[CrossRef](#)]
19. Yoshimitsu, Y.; Yasuhiro, K.; Masami, U. Induction of adiponectin by natural and synthetic phenolamides in mouse and human preadipocytes and its enhancement by docosahexaenoic acid. *Life Sci.* **2008**, *82*, 290–300. [[CrossRef](#)]
20. Muramatsu, W.; Hattori, T.; Yamamoto, H. Amide bond formation: Beyond the dilemma between activation and racemization. *Chem. Commun.* **2021**, *57*, 6346. [[CrossRef](#)]

21. Marco, T.S.; Boulton, L.T.; Sneddon, H.F.; Sheppard, T.D. A green chemistry perspective on catalytic amide bond formation. *Nat. Catal.* **2019**, *2*, 10–17. [[CrossRef](#)]
22. Munetaka, K.; Kazuhito, H.; Ayako, W.; Hiroko, K.; Shohei, T. Approach to green chemistry of DMT-MM: Recovery and recycle of coproduct to chloromethane-free DMT-MM. *Tetrahedron Lett.* **2002**, *43*, 3323–3326. [[CrossRef](#)]
23. Munetaka, K.; Kazuyoshi, Y.; Yasunobu, W.; Kazuhito, H.; Shohei, T. Development of novel polymer-type dehydrocondensing reagents comprised of chlorotriazines. *Chem. Commun.* **2005**, *21*, 2698–2700. [[CrossRef](#)]
24. Munetaka, K.; Kazuyoshi, Y.; Kazuhito, H.; Tomohito, K.; Masumi, H.; Shohei, T. Development of chlorotriazine polymer dehydrocondensing reagents (Poly-Trzs). *Tetrahedron* **2007**, *63*, 2604–2612. [[CrossRef](#)]
25. Driller, K.M.; Prateptongkum, S.; Jackstell, R.; Beller, M. A general and selective iron-catalyzed aminocarbonylation of alkynes: Synthesis of acryl- and cinnamides. *Angew. Chem. Int. Ed. Engl.* **2011**, *50*, 537–541. [[CrossRef](#)]
26. Ishihara, K.; Lua, Y. Boronic acid-DMAPO cooperative catalysis for dehydrative condensation between carboxylic acids and amines. *Chem. Sci.* **2016**, *7*, 1276–1280. [[CrossRef](#)]
27. Gualtierotti, J.B.; Schumacher, X.; Fontaine, P.; Masson, G.; Wang, Q.; Zhu, J. Amidation of aldehydes and alcohols through alpha-iminonitriles and a sequential oxidative three-component Strecker reaction/thio-Michael addition/alumina-promoted hydrolysis process to access beta-mercaptoamides from aldehydes, amines, and thiols. *Chem. Eur. J.* **2012**, *18*, 14812–14819. [[CrossRef](#)]
28. Prasad, V.; Kale, R.R.; Mishra, B.B.; Kumar, D.; Tiwari, V.K. Diacetoxyiodobenzene Mediated One-Pot Synthesis of Diverse Carboxamides from Aldehydes. *Org. Lett.* **2012**, *4*, 2936–2939. [[CrossRef](#)]
29. Li, Y.; Li, J.; Bao, G.; Yu, C.; Liu, Y.; He, Z.; Wang, P.; Ma, W.; Xie, J.; Sun, W.; et al. NDTP Mediated Direct Rapid Amide and Peptide Synthesis without Epimerization. *Org. Lett.* **2022**, *24*, 1169–1174. [[CrossRef](#)]
30. Yoon, S.; Patil, M.D.; Sarak, S.; Jeon, H.; Kim, G.-H.; Khobragade, T.P.; Sung, S.; Yun, H. Deracemization of Racemic Amines to Enantiopure (R)- and (S)-amines by Biocatalytic Cascade Employing  $\omega$ -Transaminase and Amine Dehydrogenase. *ChemCatChem* **2019**, *11*, 1898–1902. [[CrossRef](#)]
31. Bavandi, H.; Shahedi, M.; Habibi, Z.; Yousefi, M.; Brask, J.; Mohammadi, M. Biocatalytic decarboxylative Michael addition for synthesis of 1,4-benzoxazinone derivatives. *Sci. Rep.* **2022**, *12*, 12713. [[CrossRef](#)] [[PubMed](#)]
32. Simić, S.; Zukić, E.; Schmermund, L.; Faber, K.; Winkler, C.K.; Kroutil, W. Shortening Synthetic Routes to Small Molecule Active Pharmaceutical Ingredients Employing Biocatalytic Methods. *Chem. Rev.* **2022**, *122*, 1052–1126. [[CrossRef](#)] [[PubMed](#)]
33. Hanefeld, U.; Hollmann, F.; Paul, C.E. Biocatalysis making waves in organic chemistry. *Chem. Soc. Rev.* **2022**, *51*, 594–627. [[CrossRef](#)] [[PubMed](#)]
34. Petchey, M.R.; Grogan, G. Enzyme-catalyzed Synthesis of Secondary and Tertiary Amides. *Adv. Synth. Catal.* **2019**, *361*, 3895–3914. [[CrossRef](#)]
35. Burke, A.J.; Burke, A.J.; Birmingham, W.R.; Zhuo, Y.; Thorpe, T.W.; Costa, B.Z.; Crawshaw, R.; Rowles, I.; Finnigan, J.D.; Young, C.; et al. An Engineered Cytidine Deaminase for Biocatalytic Production of a Key Intermediate of the COVID-19 Antiviral Molnupiravir. *J. Am. Chem. Soc.* **2022**, *144*, 3761–3765. [[CrossRef](#)]
36. Sabi, G.J.; Gama, R.S.; Fernandez-Lafuente, R.; Cancino-Bernardi, J.; Mendes, A.A. Decyl esters production from soybean-based oils catalyzed by lipase immobilized on differently functionalized rice husk silica and their characterization as potential biolubricants. *Enzyme Microb. Technol.* **2022**, *157*, 110019. [[CrossRef](#)]
37. Holm, H.C.; Cowan, D. The evolution of enzymatic interesterification in the oils and fats industry. *Eur. J. Lipid Sci. Technol.* **2008**, *110*, 679–691. [[CrossRef](#)]
38. He, J.; Hong, B.; Lu, R.; Zhang, R.; Fang, H.; Huang, W.; Bai, K.; Sun, J. Separation of saturated fatty acids from docosahexaenoic acid-rich algal oil by enzymatic ethanolysis in tandem with molecular distillation. *Food Sci. Nutr.* **2020**, *8*, 2234–2241. [[CrossRef](#)]
39. Jiang, Y.; Gu, H.; Zhou, L.; Cui, C.; Gao, J. Novel in Situ Batch Reactor with a Facile Catalyst Separation Device for Biodiesel Production. *Ind. Eng. Chem. Res.* **2012**, *51*, 14935–14940. [[CrossRef](#)]
40. Wang, Z.-Y.; Bi, Y.-H.; Yang, R.-L.; Zhao, X.-J.; Jiang, L.; Ding, C.-X.; Zheng, S.-Y. Highly efficient enzymatic synthesis of novel polydatin prodrugs with potential anticancer activity. *Process Biochem.* **2017**, *52*, 209–213. [[CrossRef](#)]
41. Lee, J.; Kim, K.; Son, J.; Lee, H.; Song, J.H.; Lee, T.; Jeon, H.; Kim, H.S.; Park, S.J.; Yoo, H.Y.; et al. Improved Productivity of Naringin Oleate with Flavonoid and Fatty Acid by Efficient Enzymatic Esterification. *Antioxidants* **2022**, *11*, 242. [[CrossRef](#)] [[PubMed](#)]
42. Zeng, F.; Zhang, H.K.; Xu, M.M.; Huang, K.D.; Zhang, T.; Duan, J.N. Immobilized lipase catalytic synthesis of phenolamides and their potential against  $\alpha$ -glucosidase. *J. Biotechnol.* **2021**, *334*, 51–57. [[CrossRef](#)] [[PubMed](#)]
43. Sheldon, R.A.; Woodley, J.M. Role of Biocatalysis in Sustainable Chemistry. *Chem. Rev.* **2018**, *118*, 801–838. [[CrossRef](#)] [[PubMed](#)]
44. Ferlin, F.; Lanari, D.; Vaccaro, L. Sustainable flow approaches to active pharmaceutical ingredients. *Green Chem.* **2020**, *22*, 5937–5955. [[CrossRef](#)]
45. Du, L.H.; Dong, Z.; Long, R.J.; Chen, P.F.; Xue, M.; Luo, X.P. The convenient Michael addition of imidazoles to acrylates catalyzed by Lipozyme TL IM from *Thermomyces lanuginosus* in a continuous flow microreactor. *Org. Biomol. Chem.* **2019**, *17*, 807. [[CrossRef](#)]
46. Du, L.H.; Xue, M.; Yang, M.J.; Pan, Y.; Zheng, L.Y.; Ou, Z.M.; Luo, X.P. Ring-Opening of Epoxides with Amines for Synthesis of  $\beta$ -Amino Alcohols in a Continuous-Flow Biocatalysis System. *Catalysts* **2020**, *10*, 1419. [[CrossRef](#)]
47. Du, L.H.; Yang, M.J.; Pan, Y.; Zheng, L.Y.; Zhang, S.Y.; Sheng, Z.K.; Chen, P.F.; Luo, X.P. Continuous Flow Biocatalysis: Synthesis of Coumarin Carboxamide Derivatives by Lipase TL IM from *Thermomyces lanuginosus*. *Catalysts* **2022**, *12*, 339. [[CrossRef](#)]

48. DiCosimo, R.; McAuliffe, J.; Poulouse, A.J.; Bohlmann, G. Industrial use of immobilized enzymes. *Chem. Soc. Rev.* **2013**, *42*, 6437–6474. [[CrossRef](#)]
49. Carvalho, W.C.A.; Luiz, J.H.H.; Fernandez-Lafuente, R.; Hirata, D.B.; Mendes, A.A. Eco-friendly production of trimethylolpropane triesters from refined and used soybean cooking oils using an immobilized low-cost lipase (Eversa<sup>®</sup> Transform 2.0) as heterogeneous catalyst. *Biomass Bioenergy* **2021**, *155*, 106302. [[CrossRef](#)]
50. Zhang, K.P.; Lai, J.Q.; Huang, Z.L.; Yang, Z. Penicillium expansum lipase-catalyzed production of biodiesel in ionic liquids. *Bioresour. Technol.* **2011**, *102*, 2767–2772. [[CrossRef](#)]
51. Mendoza-Ortiz, P.A.; Gama, R.S.; Gómez, O.C.; Luiz, J.H.H.; Fernandez-Lafuente, R.; Cren, E.C.; Mendes, A.A. Sustainable Enzymatic Synthesis of a Solketal Ester—Process Optimization and Evaluation of Its Antimicrobial Activity. *Catalysts* **2020**, *10*, 218. [[CrossRef](#)]
52. Bansode, S.R.; Rathod, V.K. An intensified technique for lipase catalysed amide synthesis. *Chem. Eng. Process. Process Intensif.* **2019**, *143*, 107605. [[CrossRef](#)]
53. Guedes Júnior, J.G.E.; Mattos, F.R.; Sabi, G.J.; Carvalho, W.C.A.; Luiz, J.H.H.; Cren, É.C.; Fernandez-Lafuente, R.; Mendes, A.A. Design of a sustainable process for enzymatic production of ethylene glycol diesters via hydroesterification of used soybean cooking oil. *J. Environ. Chem. Eng.* **2022**, *10*, 107062. [[CrossRef](#)]
54. Lin, H.H.; Cheng, Y.; Huo, J.; Shanks, B.H. Selective Ammonolysis of Bioderived Esters for Biobased Amide Synthesis. *ACS Omega* **2021**, *6*, 30040–30049. [[CrossRef](#)]
55. de Araujo-Silva, R.; Vieira, A.C.; de Campos Giordano, R.; Fernandez-Lafuente, R.; Tardioli, P.W. Enzymatic Synthesis of Fatty Acid Isoamyl Monoesters from Soybean Oil Deodorizer Distillate: A Renewable and Ecofriendly Base Stock for Lubricant Industries. *Molecules* **2022**, *27*, 2692. [[CrossRef](#)]
56. Benítez-Mateos, A.I.; Contente, M.L.; Roura Padrosa, D.; Paradisi, F. Flow biocatalysis 101: Design, development and applications. *React. Chem. Eng.* **2021**, *6*, 599–611. [[CrossRef](#)]
57. Coloma, J.; Guiavarc'h, Y.; Hagedoorn, P.L.; Hanefeld, U. Immobilisation and flow chemistry: Tools for implementing biocatalysis. *Chem. Commun.* **2021**, *57*, 11416–11428. [[CrossRef](#)]
58. Boodhoo, K.V.K.; Flickinger, M.C.; Woodley, J.M.; Emanuelsson, E.A.C. Bioprocess intensification: A route to efficient and sustainable biocatalytic transformations for the future. *Chem. Eng. Process. Process Intensif.* **2022**, *172*, 108793. [[CrossRef](#)]
59. Sen, N.; Singh, K.K.; Mukhopadhyay, S.; Shenoy, K.T. Solvent-Free Synthesis of [DMIM]DMP Ionic Liquid in a Microreactor and Scale-Up Aspects. *Ind. Eng. Chem. Res.* **2022**, *61*, 2973–2985. [[CrossRef](#)]
60. Stradomska, D.; Coloma, J.; Hanefeld, U.; Szymańska, K. Continuous flow for enantioselective cyanohydrin synthesis. *Catal. Sci. Technol.* **2022**, *12*, 3356–3362. [[CrossRef](#)]
61. Kiviranta, P.H.; Salo, H.S.; Leppanen, J.; Rinne, V.M.; Kyrylenko, S.; Kuusisto, E.; Suuronen, T.; Salminen, A.; Poso, A.; Lahtela-Kakkonen, M.; et al. Characterization of the binding properties of SIRT2 inhibitors with a N-(3-phenylpropenoyl)-glycine tryptamide backbone. *Bioorganic Med. Chem.* **2008**, *16*, 8054–8062. [[CrossRef](#)] [[PubMed](#)]
62. Padrosa, D.R.; Contente, M.L. Multi-gram preparation of cinnamoyl tryptamines as skin whitening agents through a chemo-enzymatic flow process. *Tetrahedron Lett.* **2021**, *86*, 153453. [[CrossRef](#)]
63. Takao, K.; Toda, K.; Saito, T.; Sugita, Y. Synthesis of Amide and Ester Derivatives of Cinnamic Acid and Its Analogs: Evaluation of Their Free Radical Scavenging and Monoamine Oxidase and Cholinesterase Inhibitory Activities. *Chem. Pharm. Bull.* **2017**, *65*, 1020–1027. [[CrossRef](#)] [[PubMed](#)]
64. Chen, L.; Jin, Y.; Chen, H.; Sun, C.; Fu, W.; Zheng, L.; Lu, M.; Chen, P.; Chen, G.; Zhang, Y.; et al. Discovery of caffeic acid phenethyl ester derivatives as novel myeloid differentiation protein 2 inhibitors for treatment of acute lung injury. *Eur. J. Med. Chem.* **2018**, *143*, 361–375. [[CrossRef](#)]
65. Wang, X.; Li, Z.; Zhu, X.; Mao, H.; Zou, X.; Kong, L.; Li, X. Features and applications of reactions of  $\alpha,\beta$ -unsaturated N-acylbenzotriazoles with amino compounds. *Tetrahedron* **2008**, *64*, 6510–6521. [[CrossRef](#)]
66. Song, J. Synthesis and Anti-Itch Activity Evaluation of 5-Methoxytryptamine Derivatives. *Guangzhou Chem. Ind.* **2012**, *40*, 92–94.